



POTENTIAL TOXICITY OF *INDIGOFERA TINCTORIA* SYNTHESIZED IRON NANOPARTICLES AGAINST *Aedes Aegypti*

AYISHA CHITHIGA¹ AND KANNAYIRAM MANIMEGALAI^{1*}

¹Department of Zoology, Avinashilingam Institute for Home Science and Higher Education for Women, Coimbatore 641043, Tamil Nadu, India

*Email: manijeysu@gmail.com (corresponding author): ORCID ID 0000-0001-8627-5336

ABSTRACT

Mosquitoes are the most important single category of insects, killing millions of people worldwide each year by spreading a variety of diseases. The principal dengue vector *Aedes aegypti*, is expected to infect 2.5 billion people worldwide, or more than 40% of the world's population. According to a WHO survey, 50-100 million cases are reported globally each year. Extensive fumigation of synthetic pesticides to control the mosquito vector in Pakistan during each post-monsoon season greatly increased environmental contamination and the loss of beneficial insects from urban environments. This study looked into the larvicidal and pupicidal efficiency of green synthesized iron nanoparticles against *Ae. aegypti*. Nanoparticles were subjected to several analyses, including UV-Vis, FTIR, FESEM, EDAX, XRD, Zeta Potential, and DLS. *Ae. aegypti*, the predominant dengue mosquito, was studied for its larvicidal and pupicidal activities. *Indigofera tinctoria* produced iron nanoparticles with LC₅₀ values ranging from 4.468 ppm (I instar larvae) to 7.952 ppm (pupae). Laboratory experimental studies on larval body tissues, particularly fat cells, fingernail skin and midgut have been carried out. It has been determined the plant synthesis of iron nanoparticles are harmful to *Ae. aegypti* larval.

Key words: Dengue vector, *Aedes aegypti* nanotechnology, medicinal plant, larvicidal, histology, *Indigofera tinctoria*, morphological analysis, fluorescence, biosynthesis, green nanoparticles.

Mosquitoes serve millions of people worldwide by acting as vectors for a variety of illnesses such as dengue fever, malaria, and filariasis (Benelli, 2015). They are vulnerable vectors of several important infections, including the *Anopheles*, *Aedes*, and *Culex* genera, which include many viruses, protozoa, and nematode pathogens (Zargham et al., 2023). Dengue haemorrhagic fever, for example, has impacted over half of the world's population in the previous few decades (Messina et al., 2019; Girard et al., 2020; Brito et al., 2021). Over the last 40 years, there has been a 23 million increase in infections across 195 countries and territories, with 100 million persons infected by the end of 2017, predominantly in tropical and subtropical regions (Zeng et al., 2021). Over 960 to 4032 dengue stroke deaths among the younger generation had been recorded between 2000 and 2015 (WHO, 2022), resulting in a global public economic effect (Thompson et al., 2020). As a result of the high transmissibility of these diseases by *Aedes* mosquitoes capable of transmitting them simultaneously with a single bite (Rees et al., 2018; dos Santos Correia et al., 2023), it has become a global public health concern.

Synthetic insecticides are the first line of defence

due to their quick action; nevertheless, continuing use of synthetic insecticides may result in the development of resistance and a persistent residual effect on environment, which may be detrimental to people and include non-targeted organisms (Dusfour et al., 2019). To reduce this, it is critical to seek out biodegradable pesticide alternatives (Pathak et al., 2022; Baeshen and Baz, 2023). Green nanoparticle production is a useful, feasible, and far more potent technique for mosquito vector control (Vivekanandhan et al., 2018). Phytochemicals play a critical role in nanoparticle amalgamation, which is a green approach (Demirezen et al., 2019). Plant-mediated NP manufacturing is environmentally friendly and beneficial over synthetic chemical approaches because to its targeted applicability, low cost, single-step process, and lack of energy or temperature requirements (Benelli et al., 2017). *Indigofera tinctoria* is a plant in the Fabaceae family that is commonly known as Neeli in Tamil and is distributed throughout India. It is hepatoprotective, diuretic, and hair growth-promoting drug in the treatment of cancer, epilepsy, neuropathy, chronic bronchitis, asthma, ulcers, and skin problems (Srinivasan et al., 2016). This study evaluates the larvicidal and pupicidal activities of FeO NPs synthesized by *I. tinctoria* for

acute toxicity against *Ae. aegypti*. UV-Vis, FTIR, XRD, SEM, EDX, XRD, Zeta Potential, and DLS analysis were used to validate the quick and low-cost synthesis of FeO NPs. The dengue vector *Ae. aegypti* larvae and pupae were subjected to synthetic FeO NPs generated from *I. tinctoria* extract, and biosynthesized FeO NPs were used.

MATERIALS AND METHODS

The leaf plant of *I. tinctoria* was taken from the Western Ghats region of The Nilgiris, Southern India. The materials were washed, shade dried, crushed to a fine powder, and kept in a sterile container for future research. For 24 hr, 6 g of plant powder was incubated in 100 ml of deionized water. The plant was then filtered, and the extract was employed to create nanoparticles as a stabilizing agent. 10 g of coarse plant powder was combined with ethanol solvents and hydro macerated for three days. Continuous stirring was performed during the maceration period and was treated as a 1% stock solution. Experiment concentrations were made using this stock solution. The leaf extract was made by combining 10 g of washed and finely chopped leaves in a 300-ml Erlenmeyer flask with 100 ml of sterilized double distilled water and boiling the mixture for 5 min before decanting it. The extract was filtered using Whatman filter paper no. 1, kept at 4 °C for 5 days, and then assayed. In an Erlenmeyer flask, the filtrate was treated with aqueous 1-mM Fe₃O₄ solution and incubated at room temperature. A brown-yellow solution suggested the development of FeO NP, because the *I. tinctoria* extract decreased aqueous iron ions, resulting in stable FeO NP in water. The morphological and physiochemical properties of the biosynthesized FeO NPs were confirmed by UV-visible spectra analysis of the reaction mixture and characterization using various techniques such as FESEM and EDAX; XRD analysis was used to investigate the phase purity of the biosynthesized FeO NPs. FTIR spectroscopy was used to determine particle size and relative functional groups (Ramimoghdam et al., 2013). The particle analyzer Malvern Zetasizer nanosizer was used to measure the size of biosynthesized FeO NPs by detecting the size-dependent fluctuation of laser light scattering on bio-synthesized FeO NPs. Finally, DLS analysis was performed on the biosynthesized FeO NPs.

The eggs of mosquito were received from the National Centre for Disease Control, Mettupalayam, Coimbatore. The eggs were safely transferred to the laboratory (27± 2°C, 75–85% RH, and photoperiod by 14:10 kept in 100 ml clean water until hatching).

The mosquito larvae were provided with dog biscuits (Pedigree, USA) and yeasts (Sigma-Aldrich, Germany). The experimental larvae and pupae were placed in 500 ml of de-chlorinated water (Sujitha et al., 2015). As described by Rajaganesh et al. (2016), 25 Nos. of *Ae. aegypti* larvae (I, II, III, IV instar) and pupae were taken in a 500-ml glass beaker containing 250 ml of dechlorinated water and the optimized concentration of plant extract based FeO NPs. 0.5 mg of larval food was supplied for each test concentration. All concentrations were repeated 5 times against all instars. A separate beaker containing 250 ml of dechlorinated water and 25 Nos. of larvae and pupae served as control. The transferred larvae were treated with varying convergences of biosynthesized nanomaterials over a 24 hr incubation period, and the treated and untreated larval body images were viewed using a stereomicroscope.

The following approaches were used to treat and control *Ae. aegypti* larvae in the laboratory with FeO NPs (Kjanijou et al., 2012). Larvae were treated with LC₅₀ concentrations (ppm) for 24 hr of exposure and laboratory investigations. The larvae were fixed in 10% buffered formaldehyde for 24 hr before being dehydrated in ethanol. The nanoparticles-treated larvae were embedded in melted paraffin with glass blades in a rotary microtome at the embedding section. The section was stained with haematoxylin and eosin and photographed under a photomicroscope. FITC-labeled biosynthesized FeO NPs were used to study nanoparticle biodistribution. Following the approach described earlier (Ge et al., 2009), FITC-labeled biosynthesized FeO NPs were produced. In each well of a 24-well plate containing 1 ml of nuclease-free water, 10 mosquito larvae were inserted. FITC-biosynthesized FeO NPs were mixed uniformly with mosquito larval feeding (dog biscuit) before being implanted in 1% melted agarose. Under laboratory conditions, mosquito larvae were fed a food pellet. After 24 hr, the whole larvae were examined under a fluorescent microscope at less than 4x magnification. SPSS program (Version, 16.0) was used for all analyses. Mosquito toxicity analysis was done by probit analysis by calculating LC₅₀ and LC₉₀ as described by Finney (1971). A probability value of p<0.05 was used for the significance of differences between the obtained values.

RESULTS AND DISCUSSION

The biosynthesis of FeO NPs was confirmed within 120 min and, after that the *I. tinctoria* leaf extract synthesized FeO NPs nanoparticle a band around 310

nm (Fig. 1). Studies from Esam and AL-Kalifawi (2015) reported the magnetite iron oxide nanoparticles in the aqueous Al- Abbas's (A.S.) Hund fruit extract with absorption peaks at wavelengths of 340 nm indicating the formation of magnetite iron nanoparticles. The FTIR measurements were carried out to identify the possible biomolecules responsible for the reduction of Fe ions and capping of the reduced iron oxide nanoparticles. FTIR spectrum of FeO NPs prepared from the *I. tinctoria* leaf extract showed in the range 500-4000 cm^{-1} . The intensity peaks are slightly increased for the period of FeO NPs synthesis like 3413 cm^{-1} as well as some intensity peaks decreased like 2678, 1432, 1114 and 909 cm^{-1} (Fig. 2). The presence of active functional groups in leaf extract in the swift reduction of iron ions to iron nanoparticles. Recently, The spectra of the seaweed *K. alvarezii* extract revealed strong absorption bands at 3439, 2916, 1636, 1227, 1064, 930, 848, and 704 cm^{-1} , while the absorption bands of synthesized Fe_3O_4 -NPs were observed at 3411, 2917, 1633, 1228, 1065, 928, 846, 556, and 423 cm^{-1} (Yew et al., 2016). The morphological structure of the biosynthesized FeO NPs was studied through scanning electron microscopy (FESEM) (Fig. 3a, b). These showed different shapes of

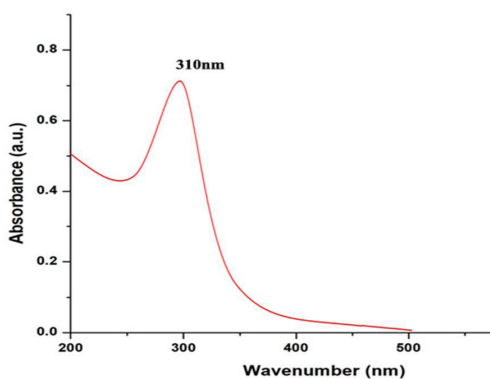


Fig. 1. UV- vis absorption spectra of iron nanoparticles synthesized using *I. tinctoria* leaf extract

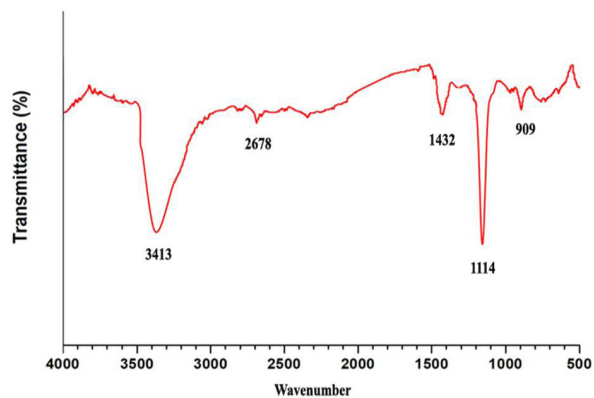


Fig. 2. FTIR spectrum of iron nanoparticles synthesized by *I. tinctoria* leaf extract

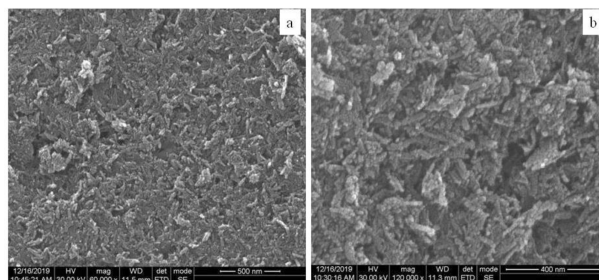


Fig. 3(a, b). SEM micrograph showing the morphological characteristics of iron nanoparticles synthesized using leaves of *I. tinctoria* leaf extract

I. tinctoria -synthesized FeO NPs, including spherical, round and hexagonal ones, with size ranging from 35 to 40 nm. The EDX spectrum recorded from *I. tinctoria* synthesized FeO NPs revealed a distinct signal and high atomic percent values for iron (Fig. 4). It implies that the nanoparticles are indeed made up of only Fe and O (Noruzi et al., 2012). Thus, the magnetite nanoparticles were successfully synthesized by this green method using *I. tinctoria* leaves extract as stabilizer for nanoparticles.

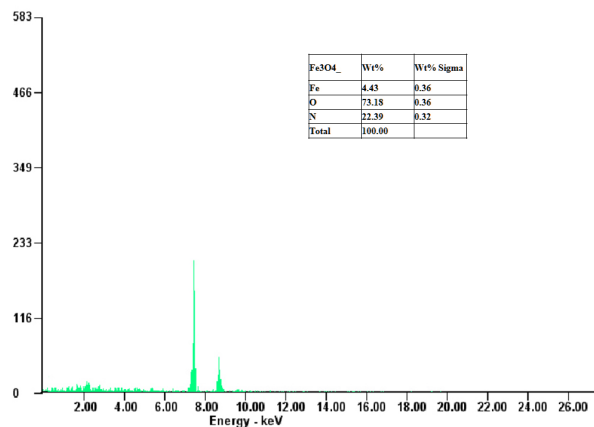


Fig. 4. EDS spectrum of *I. tinctoria* synthesized iron nanoparticles

The phase purity and crystallinity of the *I. tinctoria* synthesized FeO NPs can be identified via XRD analysis. XRD patterns showed intense peaks corresponding to the (220), (311), (222), (511) and (440) sets of lattice planes (Fig. 5). The sharp Bragg peaks reported above might have resulted due to the capping agents stabilizing the nanoparticles. Therefore, XRD results suggest that crystallization of the bio-organic phase occurred on the surface of the FeO NPs. The presence of Fe in nano powder synthesized by Gardenia leaf extract was confirmed by a series of reflection angles (2θ) at 44.34° and 64.43° having hkl values (111), (200) and (202) (Farrukh et al., 2013), respectively. Zeta potential (ZP) observed a value of +19 mV for *I. tinctoria* extract synthesized FeO NPs showed that it is constant due to

the electrostatic repulsive force. Fig. 6 and 7 represent the hydrodynamic size distribution of the FeO nanoparticles determined by dynamic laser scattering (DLS) method. The size distribution of the iron nanoparticles was found

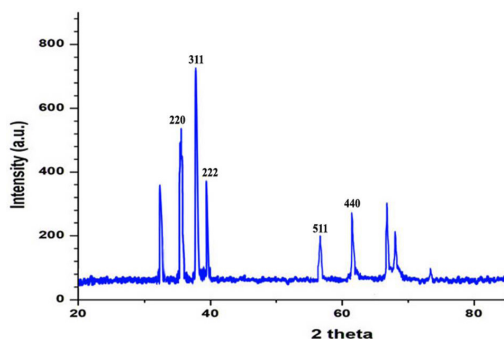


Fig. 5. XRD pattern of the *I. tinctoria* synthesized iron nanoparticles

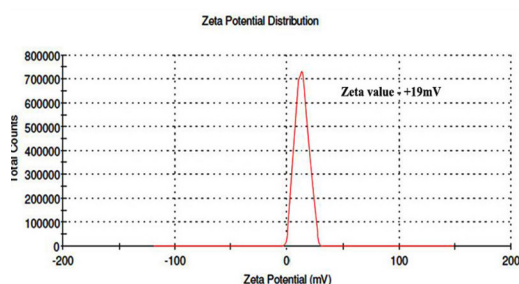


Fig. 6. Zeta Potential of *I. tinctoria* synthesised iron nanoparticles

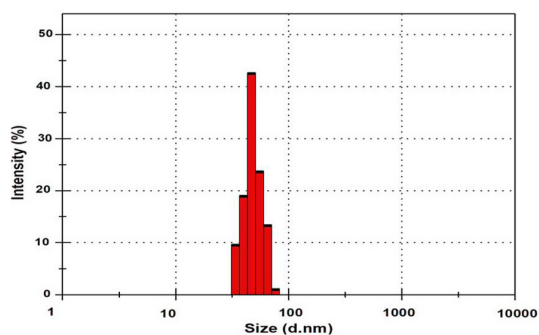


Fig. 7. DLS analysis of *I. tinctoria* synthesized iron nanoparticles

to be 80 nm. The slender increase in the hydrodynamic size confirms the significant colloidal stability of the green synthesis iron nanoparticles. The FeO particles were very heterogeneous in shape and size, ranging from structures smaller than 100 nm to angular particles several micrometers in length as shown in the SEM images.

In laboratory conditions, the *I. tinctoria* -synthesized FeO NPs were highly toxic against *Ae. aegypti* larvae and pupae; LC_{50} values ranged from 4.468 ppm (I instar), 5.134 ppm (II instar), 5.913 ppm (III instar), 6.819 ppm (IV instar), 7.952 (pupae) ppm (Table 1). The metaphor of nanoparticles treating and untreated larvae are shown in Fig. 8 (a to f). In the results observed of the untreated larvae (a) and nanoparticles treated larvae (b, c, d, e and f), it can be noticed that the biosynthesized iron nanoparticle have extremely penetrated into the larval body. Untreated larvae were observed with no morphological changes. Study on in-vivo biodistribution of and the internalization of FITC tagged FeO nanoparticles in mosquito larvae was using fluorescence microscopic analysis. At 24 hr post feeding complete larvae viewed under fluorescence microscope showed clear green signals of FITC tagged nanoparticles in all parts of the larval body especially

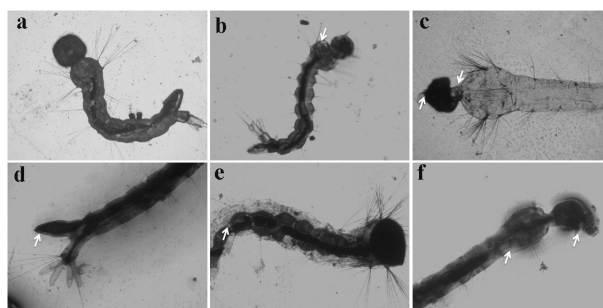


Fig. 8. Morphological analysis of *Indigofera tinctoria* synthesized iron nanoparticles on mosquito larvae; (a) shows the untreated mosquito larvae; b, c, d, e and f shows the FeO NPs treated mosquito larvae

Table 1. Larval and pupal toxicity of *Indigofera tinctoria* synthesized iron nanoparticles against the dengue vector, *Aedes aegypti*

Larval and pupal stage	LC_{50} (LC_{90})	95% confidence limit LC_{50} (LC_{90})		Regression equation	χ^2 ($d.f.=4$)
		Lower	Upper		
Larva I	4.468 (8.465)	3.197 (7.190)	5.455 (11.035)	$x=0.321 y=-1.433$	6.773 n.s
Larva II	5.134 (9.464)	3.917 (8.035)	6.185 (12.418)	$x=0.296 y=-1.520$	6.692 n.s
Larva III	5.913 (11.051)	5.423 (10.149)	6.400 (12.303)	$x=0.249 y=-1.475$	1.615 n.s
Larva IV	6.819 (12.725)	6.275 (11.519)	7.415 (14.491)	$x=0.217 y=-1.479$	0.988 n.s
Pupae	7.952 (14.686)	7.298 (13.037)	8.780 (17.261)	$x=0.190 y=-1.514$	0.958 n.s

The larval mortalities are expressed as mean \pm SD of five replicates. Nil mortality was observed in the control. Within a column means followed by the same letter(s) are not significantly different at 5% level by Duncan's multiple range test. LFL - Lower Fiducial Limit; UFL - Upper Fiducial Limit. χ^2 , Chi-square value. *Significant at $p<0.05$ level, n.s. = not significant ($\alpha=0.05$).

intestinal region (Fig. 9b-f). Simultaneously no green signals were observed from the control group (Fig. 9a). Further the green signals were also observed with fat body attached to the epidermis and midgut. Previous studies show that both positive and negatively charged nanoparticles are distributed throughout the body but negatively charged particles faster attachment than positively charged (Phanse et al., 2005).

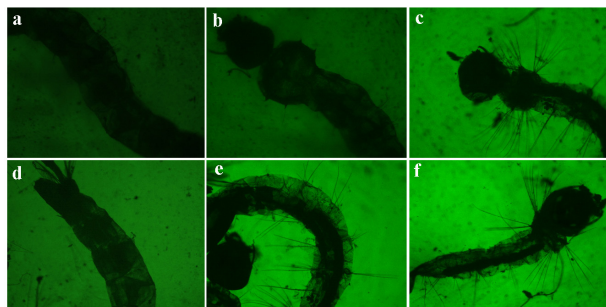


Fig. 9. Fluorescence microscope analysis of the distribution of FITC labeled *Indigofera tinctoria* synthesized iron nanoparticles in mosquito larvae; (a) shows the untreated mosquito larvae; b, c, d, e and f shows the FITC labeled FeO NPs treated mosquito larvae

The cellular and tissue damage caused by the *I. tinctoria* extract synthesized FeO NPs to *Ae. aegypti* was visualized using a light microscope by mounting cross sections of *I. tinctoria* extract synthesized nanoparticles treated *Ae. aegypti* (Fig. 10b to f). When compared to the control larvae, the histological analysis of the treated mosquito larvae clearly shows the difference and destruction caused by nanoparticles treatment (Fig. 10a). Smaller concentrations of *I. tinctoria* extract synthesized iron nanoparticles exposure lead to internal organ damage such as broken midgut, caeca, cell lysis, peritrophic membrane breakage, pre-rupturing stages of epithelial cells, and total body surface damage in mosquito larvae. Thus, a cheap aqueous extract of *I. tinctoria* leaves can be as a reducing and stabilizing agent for Fe₃O₄ nanoparticles to biosynthesize iron

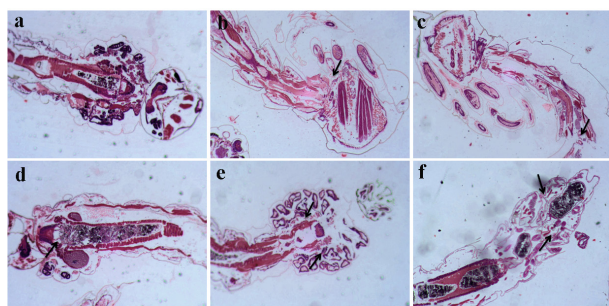


Fig. 10. Longitudinal section of *Indigofera tinctoria* synthesized iron nanoparticles on mosquito larvae; (a) shows the untreated mosquito larvae; b,c, d, e and f shows the FeO NPs treated mosquito larvae

nanoparticles. The findings indicate that *I. tinctoria*-derived FeO NPs can be proposed as effective tools for reducing larval and pupal populations. This study found that FeO NPs synthesized by *I. tinctoria* are simple to make, stable over time, and can be used at low doses.

FINANCIAL SUPPORT

This research did not received any specific grant from funding agencies.

AUTHOR CONTRIBUTION STATEMENT

Ayisha Chithiga: Study design, data collection, analysis, interpretation of results and manuscript preparation. Kannayiram Manimegalai: Drafting and conceptualization, review of literature. all authors read and approved the manuscript.

CONFLICT OF INTEREST

No conflict of interest.

REFERENCES

- Baeshen R S, Baz M M. 2023. Efficacy of *Acacia nilotica*, *Eucalyptus camaldulensis*, and *Salix safsafs* on the mortality and development of two vector-borne mosquito species, *Culex pipiens* and *Aedes aegypti*, in the laboratory and field. *Heliyon* 9(5).
- Benelli G, Caselli A, Canale A. 2017. Nanoparticles for mosquito control: Challenges and constraints. *Journal of King Saud University-Science* 29(4): 424-35.
- Brito A F, Machado L C, Oidtman R J, Siconelli M J, Tran Q M, Fauver J R, Carvalho R D, Dezordi F Z, Pereira M R, de Castro-Jorge L A, Minto E C. 2021. Lying in wait: The resurgence of dengue virus after the Zika epidemic in Brazil. *Nature communications* 12(1):2619.
- Demirezen DA, Yıldız Y Ş, Yılmaz D D. 2019. Amoxicillin degradation using green synthesized iron oxide nanoparticles: Kinetics and mechanism analysis. *Environmental Nanotechnology, Monitoring and Management* 11: 100219.
- dos Santos Correia P R, de Freitas J D, Zeoly LA, Porto R S, da Paz Lima D J. 2023. Discovery and structure-activity relationship of Morita-Baylis-Hillman adducts as larvicides against dengue mosquito vector, *Aedes aegypti* (Diptera: Culicidae). *Bioorganic and Medicinal Chemistry* 90: 117315.
- Dusfour I, Vontas J, David J P, Weetman D, Fonseca D M, Corbel V, Raghavendra K, Coulibaly M B, Martins A J, Kasai S, Chandre F. 2019. Management of insecticide resistance in the major *Aedes* vectors of arboviruses: Advances and challenges. *PLoS Neglected Tropical Diseases* 13(10): 0007615.
- Esam J A L, Kalifawi. 2015. Green synthesis of magnetite iron oxide nanoparticles by using Al-Abbas's (AS) hund fruit (*Citrus medica*) var *Sarcodactylis Swingle* extract and used in Al-'alqami river water treatment. *Journal of Natural Sciences Research* ISSN 2224-3186 (paper) ISSN 2225-0921 (Online) 5: 20.
- Farrukh M A, Ali S, Rahman M K. 2013. Photodegradation of 2,4,6-trinitrophenol catalyzed by Zn/ MgO nanoparticles prepared in aqueous-organic medium. *Korean Journal of Chemical Engineering* 30(11): 2100-2107.

- Finney D J. 1971. Probit analysis. Cambridge University Press, London. pp. 68-78.
- Ge Y, Zhang Y, He S, Nie F, Teng G, Gu, N. 2009. Fluorescence modified chitosan-coated magnetic nanoparticles for high-efficient cellular imaging. *Nanoscale Research Letters* 4(4): 287-295.
- Girard M, Nelson C B, Picot V, Gubler D J. 2020. Arboviruses: A global public health threat. *Vaccine* 38(24): 3989-94.
- Kjanijou M, Jiraungkoorskul K, Kosai P, Jiraungkoorskul W. 2012. Effect of *Murraya paniculata* leaf extract against *Culex quinquefasciatus* larva. *Asian Journal of Biological Sciences* 5(4): 201-8.
- Messina J P, Brady O J, Golding N, Kraemer M U, Wint G W, Ray S E, Pigott D M, Shearer FM, Johnson K, Earl L, Marczak L B. 2019. The current and future global distribution and population at risk of dengue. *Nature Microbiology* 4(9): 1508-15.
- Noruzi M, Zare D, Davoodi D. 2012. A rapid biosynthesis route for the preparation of gold nanoparticles by aqueous extract of cypress leaves at room temperature. *Spectrochimica Acta, Part A: Molecular and Biomolecular Spectroscopy* 94: 84-88
- Pathak V M, Verma V K, Rawat B S, Kaur B, Babu N, Sharma A, Dewali S, Yadav M, Kumari R, Singh S, Mohapatra A. 2022. Current status of pesticide effects on environment, human health and it's eco-friendly management as bioremediation: A comprehensive review. *Frontiers in Microbiology* 2833.
- Phanse Y, Dunphy B M, Perry J L, Airs P M, Paquette C C, Carlson J O, Xu J, Luft J C, DeSimone J M, Beaty B J, Bartholomay L C. 2015. Biodistribution and toxicity studies of PRINT hydrogel nanoparticles in mosquito larvae and cells. *PLoS Neglected Tropical Diseases* 9(5): 0003735.
- Rajaganesh R, Murugan K, Panneerselvam C, Jayashanthini S, Roni M, Suresh U, Trivedi S, Rehman H, Higuchi A, Nicoletti M, Benelli G. 2016. Fern-synthesized silver nanocrystals: towards a new class of mosquito oviposition deterrents?. *Research in Veterinary Science* 109:40-51.
- Rees E E, Petukhova T, Mascarenhas M, Pelcat Y, Ogden N H. 2018. Environmental and social determinants of population vulnerability to Zika virus emergence at the local scale. *Parasites and vectors* 11(1): 1-3.
- Srinivasan S, Wankhar W, Rathinasamy S, Rajan R. 2016. Free radical scavenging potential and HPTLC analysis of *Indigofera tinctoria* linn (Fabaceae). *Journal of Pharmaceutical Analysis* 6(2):125-31.
- Thompson R, Martin Del Campo J, Constenla D. 2020. A review of the economic evidence of *Aedes*-borne arboviruses and *Aedes*-borne arboviral disease prevention and control strategies. *Expert Review of Vaccines* 19(2): 143-62.
- Vivekanandhan P, Venkatesan R, Ramkumar G, Karthi S, Senthil-Nathan S, Shivakumar M S. 2018. Comparative analysis of major mosquito vectors response to seed-derived essential oil and seed pod-derived extract from *Acacia nilotica*. *International Journal of Environmental Research and Public Health* 15(2):388.
- World Health Organization. 2022. Dengue and Severe Dengue. <https://www.who.int/news-room/fact-sheets/detail/dengue-and-severe-dengue>.
- Yew Y P, Shameli K, Miyake M, Kuwano N, Bt Ahmad Khairudin N B, Bt Mohamad S E, Lee KX. 2016. Green synthesis of magnetite (Fe₃O₄) nanoparticles using seaweed (*Kappaphycus alvarezii*) extract. *Nanoscale Research Letters* 11:1-7.
- Zargham F, Afzal M, Rasool K, Manzoor S, Qureshi NA. 2023. Larvicidal activity of green synthesized iron oxide nanoparticles using *Grevillea robusta* Cunn. leaf extract against vector mosquitoes and their characterization. *Experimental Parasitology* 108586.
- Zeng Z, Zhan J, Chen L, Chen H, Cheng S. 2021. Global, regional, and national dengue burden from 1990 to 2017: A systematic analysis based on the global burden of disease study 2017. *eClinicalMedicine* 32: 100712.

(Manuscript Received: August, 2023; Revised: January, 2024;

Accepted: January, 2024; Online Published: March. 2024)

Online First in www.entosocindia.org and indianentomology.org Ref. No. e24568